

PAPER Special Section on Heterostructure Microelectronics with TWHM2005

Cubic GaN/AlGaN HEMTs on 3C-SiC Substrate for Normally-Off Operation

Masayuki ABE^{†a)}, Member, Hiroyuki NAGASAWA[†], Stefan POTTHAST^{††}, Jara FERNANDEZ^{††}, Jörg SCHÖRMANN^{††}, Donat Josef AS^{††}, and Klaus LISCHKA^{††}, Nonmembers

SUMMARY Phase pure cubic (c-) GaN/AlGaN heterostructures on 3C-SiC free standing (001) substrates have successfully been developed. Almost complete (100%) phase pure c-GaN films are achieved with 2-nm surface roughness on 3C-SiC substrate and stoichiometric growth conditions. The polarization effect in c-GaN/AlGaN has been evaluated, based on measuring the transition energy of GaN/AlGaN quantum wells (QWs). It is demonstrated that the polarization electric fields are negligible small in c-GaN/AlGaN/3C-SiC compared with those of hexagonal (h-)GaN/AlGaN, 710 kV/cm for Al content x of 0.15, and 1.4 MV/cm for x of 0.25. A sheet carrier concentration of c-GaN/AlGaN heterojunction interface is estimated to $1.6 \times 10^{12} \text{ cm}^{-2}$, one order of magnitude smaller than that of h-GaN/AlGaN. The band diagrams of c-GaN/AlGaN HEMTs have been simulated to demonstrate the normally-off mode operation. The blocking voltage capability of GaN films was demonstrated with C-V measurement of Schottky diode test vehicle, and extrapolated higher than 600 V in c-GaN films at a doping level below $5 \times 10^{15} \text{ cm}^{-3}$, to show the possibility for high power electronics applications.

key words: cubic GaN, GaN/AlGaN HEMT, piezo, spontaneous, polarization, blocking voltage

1. Introduction

GaN/AlGaN based High Electron Mobility Transistors (HEMTs) have recently attracted considerable attentions due to their potentialities for high-voltage and high power operations in power electronics as well as in microwave applications [1]. The GaN material is appealed with properties of high peak electron velocity, saturation velocity, breakdown fields and thermal stability due to its wide bandgap for such applications, and also the potential to form lattice-matched heterojunctions with other group III-nitride materials.

High frequency GaN/AlGaN HEMTs are already commercially available for base-stations of W-CDMA mobile-phone applications [2], [3]. The GaN/AlGaN HEMTs are also aggressively developed in power electronics applications [4], such as 600 V class inverters [5], DC-DC converters [6], and high current switching [7]. These are based on high electron concentration of two dimensional electron gas (2DEG) over $1 \times 10^{13} \text{ cm}^{-2}$, which is one-order of magnitude higher than that of GaAs/AlGaAs material system, due to the large polarization charge effects (spontaneous and

piezo polarization charges) at the heterojunction interface [8], [9]. These HEMT devices reported so far show mainly for normally-on mode operation.

The GaN/AlGaN HEMTs with normally-off mode operation, which are much required from the system side, however, are still under developing with demonstrations in device principle levels. Most of them are based on a hexagonal GaN (h-GaN) technology and not on a cubic GaN (c-GaN) one, in which less data, even fundamental data, are available.

This paper presents the demonstration of almost complete phase pure c-GaN/AlGaN heterostructures for the operation of cubic GaN/AlGaN HEMTs in normally-off mode, using large diameter of 3C-SiC free standing (001) substrates fabricated by HAST Co., Ltd. [10] for the epitaxy of group III-nitrides.

2. Phase Pure Cubic Group III-Nitrides

2.1 Growth of Cubic GaN, AlGaN, and AlN Layers

Cubic group III-nitride samples are grown on 200 μm thick, free standing 3C-SiC (001) substrates by plasma assisted molecular beam epitaxy (MBE) to provide activated nitrogen atoms. Aluminum and gallium were evaporated from Knudsen cells. Cubic GaN, AlGaN, and AlN layers were grown at 720°C directly on 3C-SiC substrates, controlled in-situ using the intensity of a reflected high energy electron beam (RHEED). The structural and morphological properties of both the 3C-SiC substrates and the group III-nitride epilayers were measured by high resolution X-ray diffraction (HRXRD) and atomic force microscopy (AFM). HRXRD and reciprocal space mapping (RSM) have been performed to determine the Al and Ga contents and the strain in the $\text{Al}_x\text{Ga}_{1-x}\text{N}$.

The optimum conditions for the epitaxial growth of c-GaN are mainly determined by the surface morphology of the 3C-SiC substrate and the growth conditions during epitaxy. The surface stoichiometry and the substrate temperature are important parameters. Monitoring the MBE growth process by RHEED is achieved in-situ to control of both substrate temperature and surface stoichiometry. The RMS-roughness measured by a $5 \times 5 \mu\text{m}^2$ AFM-scan is decreasing from 16 nm to a minimum value of 2.5 nm.

Manuscript received November 8, 2005.

Manuscript revised January 10, 2006.

[†]The authors are with Hoya Advanced Semiconductor Technologies (HAST) Co., Ltd., Sagamihara-shi, 229-1125 Japan.

^{††}The authors are with University of Paderborn, 33095, Paderborn, Germany.

a) E-mail: abe@hast.co.jp

DOI: 10.1093/ietele/e89-c.7.1057

2.2 Characterization of Cubic Group III-Nitrides Layer

In order to characterize cubic GaN epilayer properly, it is necessary to detect off-axis cubic and hexagonal planes tilted from the surface. Therefore reciprocal space map (RSM) or pole figure measurements are necessary to check the phase purity of the cubic GaN epilayers. The hexagonal inclusions for phase pure cubic group III-nitride films with around 600 nm thickness are obtained by measuring the X-ray intensity ratio of $I_{(10-11)\text{hex}}/I_{(002)\text{cub}}$. Figure 1 shows the dependence of the hexagonal inclusions in c-GaN, AlGaN, and AlN films on the surface roughness of the 3C-SiC substrate. Almost complete (100%) phase pure cubic GaN films are achieved with a surface roughness of 2 nm [11]. Figure 2 shows a typical reciprocal space mapping (RSM) of the (002) reflection of c-GaN/3C-SiC epilayer. As seen in this figure, the utmost RSM is measured for samples with proper growth conditions. Except for the (002) reflexes of the cubic GaN and of the 3C-SiC substrate no additional reflexes could be observed. A phase purity of better than

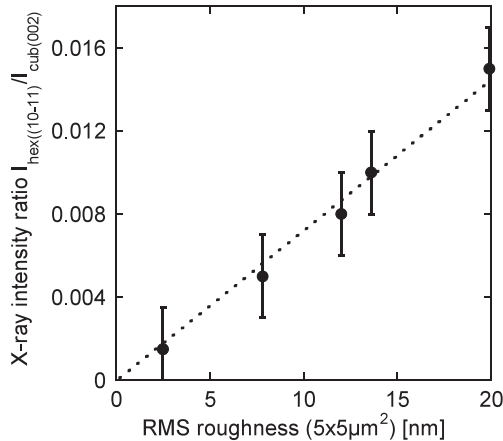


Fig. 1 Dependence of hexagonal inclusions in c-GaN, AlGaN, and AlN films on surface roughness of 3C-SiC substrate.

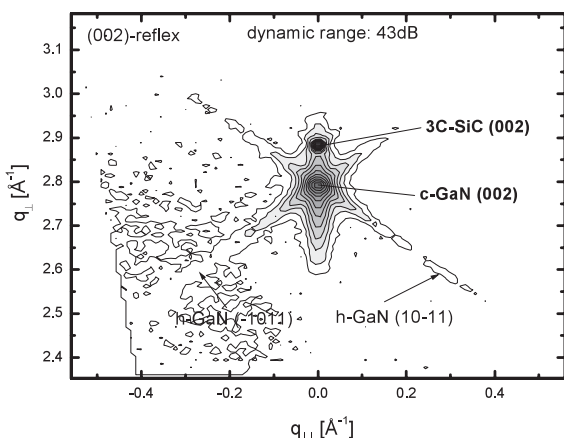


Fig. 2 Reciprocal space mapping (RSM) of (002) reflection of c-GaN/3C-SiC epilayer.

99.9% could be estimated by structural analysis [12].

3. Polarization Effects and 2DEG Concentrations

3.1 Experimental Comparisons of Cubic and Hexagonal Multi-Quantum Wells

Phase pure c-GaN/Al_xGa_{1-x}N multiple quantum wells (MQWs) were grown on GaN buffer layers. The c-GaN/Al_xGa_{1-x}N MQW consists of 5 QWs typically with a barrier and well thickness of 5 nm and 10 nm, respectively [13]. The chemical purity of the c-GaN/Al_{0.25}Ga_{0.75}N multiple quantum well (MQW) structure has been analyzed with secondary ion mass spectroscopy (SIMS) measurements. The residual impurities like O or C in both the binary semiconductor GaN and in the Al_{0.25}Ga_{0.75}N alloy and the Al content can be measured. Results are shown in Fig. 3. The profiles of N and Al have been shifted downwards in comparison to the Ga-profile. The Ga and Al-profiles nicely resemble the actual MQW structure, which is schematically drawn on the right side of Fig. 3. The five GaN quantum wells can clearly be identified in the Ga signal exactly at the depth position expected due to the sequence of growth. From the Al signal intensity an Al content of 25% is estimated in excellent agreement with the intended Al content and the Al-content measured by X-ray reciprocal space mapping. The slight modulation of the intensity of the N profile observed at the depth of the MQW is due to the so called Matrix effects, which takes into account that the SIMS sensitivity is dependent on the surrounding material.

3.2 Polarization Effects and 2DEG Concentrations

One of the advantages of cubic group III-nitride growth in (001) direction in comparison to hexagonal GaN grown either on sapphire (c-axis) or on hexagonal SiC is the absence of polarization effects due to spontaneous and piezoelectric polarization. In GaN/Al_xGa_{1-x}N quantum well structures these polarization effects introduce strong electric fields in the order of MV/cm. These electric fields result in a strong red shift of the emission line due to the quantum confined

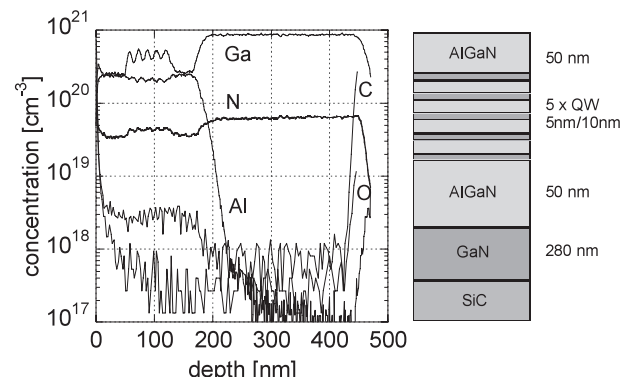


Fig. 3 Depth profile of SIMS measurement for phase pure c-AlGaN/GaN MQW structure.

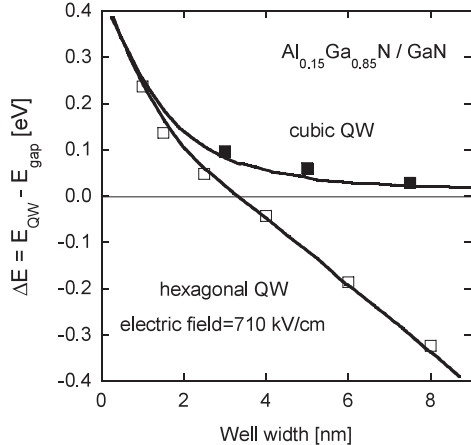


Fig. 4 Energy difference of cubic and hexagonal GaN/AlGaN QWs as a function of QW-width.

Stark effect and a spatial separation of the electron and hole wave function, which strongly reduces the quantum efficiency.

The transition energy of c-GaN/Al_xGa_{1-x}N quantum well emission is measured versus the QW width. No additional electric field has to be assumed to explain the well width dependence for cubic QWs. The transition energies of hexagonal GaN/Al_xGa_{1-x}N quantum well [14] are plotted in Fig. 4, compared with c-GaN/Al_xGa_{1-x}N quantum wells. The band gap energy of hexagonal GaN is about 3.4 eV, 0.2 eV higher than 3.2 eV of cubic GaN. The polarization effect in c-GaN/AlGaN is negligible small, as shown in Fig. 4, where the energy difference ΔE of the transition energy E_{QW} of c-GaN/AlGaN/3C-SiC QW structures to the band gap energy E_{gap} is plotted versus quantum well thickness. The transition energies E_{QW} in the hexagonal case are lower than the energy gap of hexagonal GaN, which results from a strong internal electric field in the QW (quantum confined Stark effect). This strong internal electric field is due to the spontaneous and piezoelectric fields which exists in hexagonal GaN. The strength of the electric fields increases with Al content and is about 710 kV/cm for $x=0.15$ and about 1.4 MV/cm for $x=0.25$. From this difference in the transition energies between hexagonal and cubic GaN/Al_xGa_{1-x}N QWs we can definitively exclude spontaneous polarization field in our c-GaN crystals.

A well established method to analyze heterostructures are C-V measurements which means the depth distribution of the net donor concentration $N_D - N_A$. Figure 5 shows the carrier concentration distribution of an GaN/Al_{0.3}Ga_{0.7}N heterojunction versus depth together with the simulated electron profile (full line) [15]. The C-V measurement was performed at 150 K. The depth position (60 nm) of the maximum electron concentration of about $4 \times 10^{18} \text{ cm}^{-3}$ is in excellent agreement with the simulated profile. From the 4 nm-width of the electron distribution and the peak electron concentration a sheet carrier concentration of about $1.6 \times 10^{12} \text{ cm}^{-2}$ is estimated.

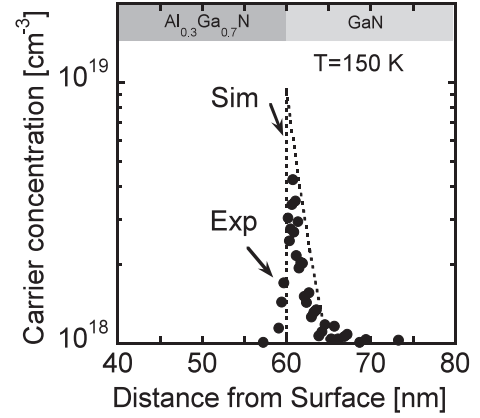


Fig. 5 Experimental and simulated carrier concentration distributions at GaN/AlGaN heterojunction interface.

4. Cubic GaN/AlGaN HEMT Devices

4.1 Breakdown Voltage Characteristics

The Schottky diode is an excellent test vehicle for measuring material quality. The thickness of the c-GaN and c-Al_{0.3}Ga_{0.7}N epilayers are about 600 nm and 30 nm, respectively. The quality of the cubic epilayers was checked by HRXRD, AFM and photoluminescence (PL). Ni/In (50 nm/150 nm) Schottky contacts of 300 μm in diameter were fabricated on c-GaN and c-GaN/Al_{0.3}Ga_{0.7}N structures, grown on 3C-SiC free standing (001) substrates as shown in detail in Ref. [10], by thermal evaporation using contact lithography. A clear rectifying behavior was measured in our SBDs and the current voltage (I - V) behavior of the device in the dark was studied in detail. Capacitance-voltage (C-V) measurements and electrochemical C-V profiling (ECV) were used to determine the net donor concentration in our cubic GaN and Al_{0.3}Ga_{0.7}N layers which varied between $9 \times 10^{16} \text{ cm}^{-3}$ to $2 \times 10^{19} \text{ cm}^{-3}$. The dependence of breakdown voltages on the doping density derived from the reverse breakdown voltage characteristics of c-GaN SBDs was investigated.

The room temperature (RT) I - V curve (full circles) of a typical Ni-Schottky contact on as-grown c-GaN is shown in Fig. 6, clearly demonstrating a rectifying characteristic. The inset shows a schematic drawing of the device structure. C-V measurements performed on the same sample gave a net donor concentration $N_D - N_A = 1.8 \times 10^{17} \text{ cm}^{-3}$. From the linear increase of the current with forward bias a series resistance of $R_S=230 \text{ Ohm}$ was obtained for the as-grown sample. By thermal annealing of the Ni contact at 200°C in ambient air the I - V characteristics were improved to the one shown by the full squares. The series resistance increased to $R_S=310 \text{ Ohm}$, and the current at reverse biases was decreased by about three orders of magnitude, as discussed in detail [16].

In Fig. 7 the reverse breakdown voltages (V_B) of c-GaN (full circles) and c-Al_{0.3}Ga_{0.7}N (full squares) Ni-SBDs ver-

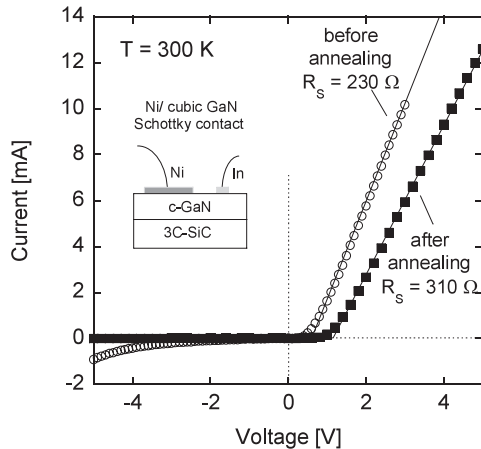


Fig. 6 Current-voltage (I - V) characteristics of a Ni-Schottky contact on c-GaN.

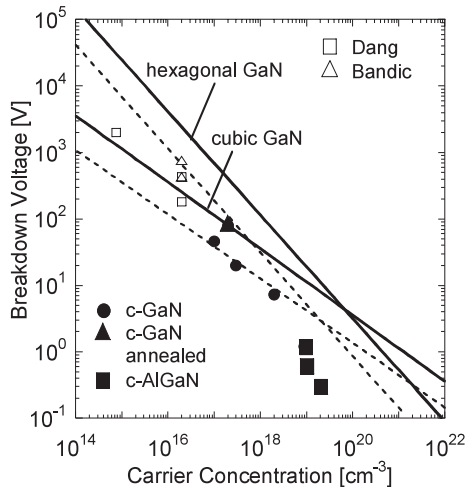


Fig. 7 Carrier concentration dependence of reverse breakdown voltage.

sus the doping density ($N_D - N_A$) measured by C-V or ECV are plotted. The full lines show the calculated doping dependence of V_B for c-GaN and h-GaN, respectively [17]. Included in Fig. 7 are also experimental data obtained on h-GaN (open squares [18] and open triangles [19]). The experimental values of V_B in c-GaN are one-third smaller than the theoretical values and show the same dependence on the doping level as in h-GaN (dashed lines). Crystal defects like dislocations or point defects may be the reason for the deviation between experimental data and theoretical calculations. This interpretation in c-GaN is supported by the experimental data obtained on the annealed sample (full triangle), where the measured V_B of 80 V at a carrier concentration of $1.8 \times 10^{17} \text{ cm}^{-3}$ is in excellent agreement with the theoretical curve. For lower breakdown voltage in c-Al_{0.3}Ga_{0.7}N epilayers (full squares), the larger deviation to the theoretical curve may be due to the structure of AlGaN/GaN, crystal defects and higher doping of around $1 \times 10^{19} \text{ cm}^{-3}$, as well as due to a higher oxygen impurities (O_N). For GaN and Al_{0.3}Ga_{0.7}N nitrogen vacancies (V_N) or

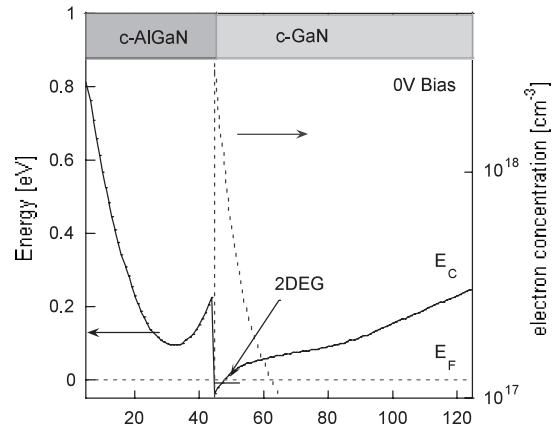


Fig. 8 Conduction band diagram and electron concentration of a c-GaN/AlGaN HEMT in normally-on mode (a) at 0 V (logical on-state) and (b) at -1.5 V (logical off-state).

O_N concentration may be the reason for the donor defects. The influence of oxygen may be more severe for Al_{0.3}Ga_{0.7}N epilayers due to the increased affinity of Al to oxygen. This is also in agreement to the observation that the leakage current is higher in Al_{0.3}Ga_{0.7}N Schottky diodes than in GaN Schottky diodes [16]. From these experimental data we extrapolate a blocking voltage of higher than 600 V in c-GaN films at a doping level below $N_D = 5 \times 10^{15} \text{ cm}^{-3}$.

4.2 Band Diagram Simulations of Cubic GaN/AlGaN HEMTs

One of the advantages of cubic group III nitrides in comparison with hexagonal group III nitrides is the absence of polarization effects as demonstrated in Sect. 3. To check the logic states and the realization of depletion-mode and enhancement-mode HEMTs with c-GaN/AlGaN structures we have simulated these structures at different applied gate voltages, using a FreeWare program called "1D Poisson" program. For the Schottky barrier we assume a gate volt-

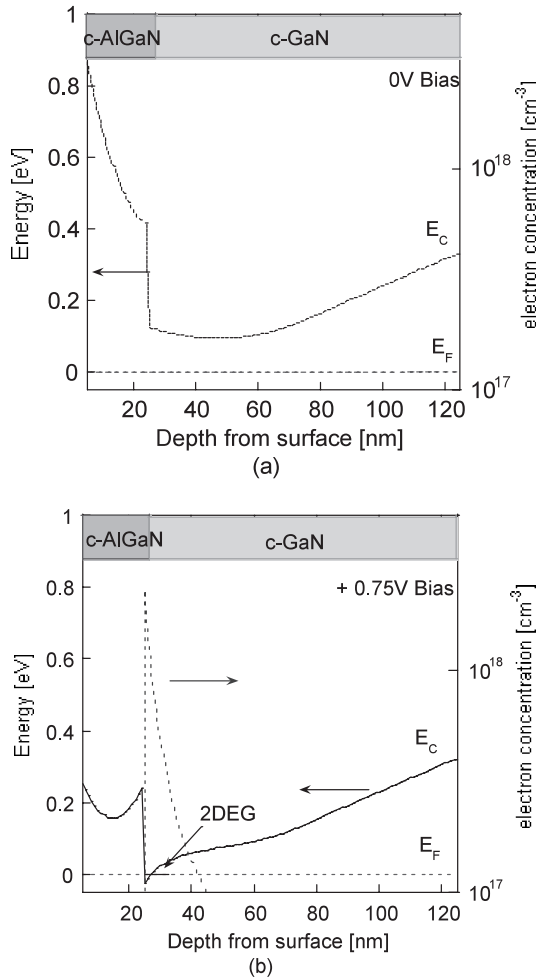


Fig. 9 Conduction band diagram and electron concentration of a c-GaN/AlGaN HEMT in normally-off mode (a) at 0 V (logical off-state) and (b) +0.75 V (logical on-state).

age of 0.8 eV as is typical for a Ni/Au contact on c-GaN. The thickness of the Al_{0.3}Ga_{0.7}N layer was 40 nm and the Al_{0.3}Ga_{0.7}N doping concentration was assumed to be 10¹⁸ cm⁻³. Figures 8(a) and 8(b) show the conduction band structures and the electron density distributions of a c-GaN/Al_{0.3}Ga_{0.7}N HEMT structure heterojunction under externally applied gate biases of 0 V and -1.5 V, respectively. A 2-dimensional electron gas (2DEG) is formed at 0 V (see carrier concentration in Fig. 8(a)), whereas at -1.5 V the 2DEG is totally depleted. Such a behavior is characteristic for a HEMT device in normally-on operation or depletion-mode. Normally-off operation or enhancement-mode devices, however, require that a positive gate bias is applied to open the channel. In cubic HEMT structures this can simply be realized by reducing the thickness of the top Al_{0.3}Ga_{0.7}N layer from 40 nm to 20 nm. The other parameters used for the simulations are the same as for the depletion-mode device. The corresponding calculations are shown in Figs. 9(a) and 9(b). Indeed at 0 V the channel is closed and at +0.75 V the channel is opened for current transport. This simulation demonstrates the applicability of c-GaN/Al_{0.3}Ga_{0.7}N for the

realization of both enhancement-mode and depletion-mode HEMT structures, as are necessary for different VLSI logics.

5. Conclusion

Phase pure c-GaN/AlGaN heterostructures were successfully developed by plasma assisted MBE on 3C-SiC free standing (001) substrates. The negligible small polarization electric field in c-GaN/AlGaN/3C-SiC has been demonstrated by evaluating the QW-width dependence of the transition energy of QWs. From the C-V characteristics of fabricated c-GaN Schottky diodes, a blocking voltage of higher than 600 V is extrapolated for c-GaN films with a doping level of 5 × 10¹⁵ cm⁻³ to show the possibility of high power electronics applications. It becomes clear from the simulated data that the c-GaN/AlGaN HEMTs on 3C-SiC substrates with normally-off mode operation could be realized with the large technological allowance and the same flexible device design ability as GaAs/AlGaAs HEMT technology.

Acknowledgement

The authors gratefully acknowledge SIMS measurements by Dr. Manfred Maier, IAF, Fraunhofer-Institute, Germany.

References

- [1] M. Abe, "A quarter century of HEMT device technology," Proc. 21st Symposium on Materials Science and Engineering, Research Center of Ion Beam Technology, pp.7–14, Hosei University, Dec. 2002.
- [2] K. Joshi, T. Kikkawa, H. Hayashi, T. Maniwa, S. Yokokawa, M. Yokoyama, N. Adachi, and M. Takikawa, "A 174 W high-efficiency GaN HEMT power amplifier for W-CDMA base station application," IEEE IEDM Tech. Digest, pp.983–985, Dec. 2003.
- [3] Y. Ando, Y. Okamoto, K. Hataya, T. Nakayama, H. Miyamoto, T. Inoue, and M. Kuzuhara, "12 W/mm recessed-gate AlGaN/GaN heterojunction field-plate FET," IEEE IEDM Tech. Digest, pp.563–566, Dec. 2003.
- [4] Z.-Q. Zhang, B. Moran, S.P. DenBaars, U.K. Mishra, X.W. Wang, and T.P. Ma, "Effects of surface traps on breakdown voltage and switching speed of GaN switching HEMTs," IEEE IEDM, pp.589–592, Dec. 2001.
- [5] S. Yoshida, J. Li, T. Wada, and H. Takehara, "High-power AlGaN/GaN HFET with a lower on-state resistance and a higher switching time for an inverter circuit," ISPSD, S3P3, 2003.
- [6] W. Saito, Y. Takada, M. Kuraguchi, K. Tsuda, I. Omura, and T. Ogura, "600 V AlGaN/GaN power-HEMT: Design, fabrication and demonstration on high voltage DC-DC converter," IEEE IEDM Tech. Digest, pp.587–590, Dec. 2003.
- [7] M. Hikita, M. Yanagihara, K. Nakazawa, H. Ueno, Y. Hirose, T. Ueda, Y. Uemoto, T. Tanaka, D. Ueda, and T. Egawa, "350 V/150 A AlGaN/GaN power HFET on silicon substrate with source-via grounding (SVG) structure," IEEE IEDM Tech. Digest, pp.803–806, Dec. 2004.
- [8] F. Sacchi, A.D. Carlo, P. Lugli, and H. Morkoc, "Spontaneous and piezoelectric polarization effects on the output characteristics of AlGaN/GaN heterojunction Modulation doped FETs," IEEE Trans. Electron Devices, vol.48, no.3, pp.450–457, 2001.
- [9] O. Ambacher, J. Majewski, C. Miskys, A. Link, M. Herman, M. Eickhoff, M. Stutzmann, F. Bernardini, V. Fiorentini, V. Tilak, B. Schaff, and L.F. Eastman, "Pyroelectric properties of

- Al(In)GaN/GaN hetero- and quantum well structures," J. Phys.: Condens. Matter, vol.14, pp.3399–3434, 2002.
- [10] H. Nagasawa, K. Yagi, T. Kawahara, N. Hatta, G. Pensl, W.J. Choyke, T. Yamada, K.M. Itoh, and A. Schoner, "Low-defect 3C-SiC grown on undulant-Si (001) substrates," in Silicon Carbide, ed. W.J. Choyke, H. Matsumani, and G. Pensl, pp.207–228, Springer, Berlin, 2003.
- [11] M. Abe, H. Nagasawa, D.J. As, and K. Lischka, "Future prospect of cubic GaN/AlGaN HEMT technology," 13th Meeting on SiC and Related Wide Bandgap Semiconductors, p.69, 2004.
- [12] M. Abe, H. Nagasawa, S. Pothast, D.J. As, and K. Lischka, "Cubic GaN/AlGaN HEMTs on 3C-SiC substrate for normally-off operation," 6th Topical Workshop on Heterostructure Microelectronics TWHM, WeB-5, 2005.
- [13] D.J. As, S. Pothast, J. Schormann, S.F. Li, K. Lischka, H. Nagasawa, and M. Abe, "Molecular beam epitaxy of cubic group III-nitrides on free-standing 3C-SiC substrates," ICSCRM, FA2. EPI IV, p.82, Sept. 2005.
- [14] N. Grandjean, B. Damilano, S. Dalmasso, M. Leroux, M. Laugt, and J. Massies, "Built-in electric-field effects in wurtzite AlGaN/GaN quantum wells," J. Appl. Phys., vol.86, no.7, pp.3714–3720, 1999.
- [15] S. Pothast, J. Schormann, J. Fernandez, D.J. As, K. Lischka, H. Nagasawa, and M. Abe, "Two dimensional electron gas in cubic $\text{Al}_x\text{Ga}_{1-x}\text{N}/\text{GaN}$ heterostructures," ICNS-6, Mo-P-087, Aug. 2005.
- [16] D.J. As, S. Pothast, J. Fernandez, K. Lischka, H. Nagasawa, and M. Abe, "Cubic GaN/AlGaN Schottky barriers devices on 3C-SiC substrates," ICMAT, K-8-OR14, July 2005.
- [17] K. Matocha, T.P. Chow, and R.J. Gutmann, "Gallium nitride power device design tradeoffs," Mat. Sci. Forum, vol.389-393, pp.1531–1534, 2002.
- [18] G.T. Dang, A.P. Zhang, M.M. Mahewa, F. Ren, J.I. Chyl, C.M. Lee, C.C. Chuo, G.C. Chi, J. Han, S.N.G. Chu, R.G. Wilson, X.A. Cao, and S.J. Pearton, "High breakdown voltage Au/Pt/GaN Schottky diodes," J. Vac. Sci. Technol. A, vol.18, no.4, pp.1135–1138, 2000.
- [19] Z.Z. Bandic, M. Bridger, E.C. Piquette, and T.C. McGill, "High voltage (450 V) GaN Schottky rectifiers," Appl. Phys. Lett., vol.74, no.9, pp.1266–1268, 1999.



Masayuki Abe received the B.E., M.E., and Ph.D. degrees in Electrical Engineering from Osaka University, Osaka, Japan, in 1967, 1969, and 1973, respectively. In 1973, he joined Fujitsu Laboratories, Ltd., Japan, where he was engaged in developing high-radiance LEDs for fiber-optics, microwave HEMTs for DBS receiver, high-speed HEMT LSIs for supercomputer, and low-temperature poly-Si TFTs for LCD flat-pans. Since 1998, he has been engaged in developing kilo-watt class power GaN

HEMTs for fuel-cell inverters, HEMT based infrared image-sensor at KRI Inc., and also 3C-SiC power MOSFETs and cubic GaN HEMTs at HOYA Advanced Semiconductor Technologies (HAST) Co., Ltd. He is currently General Manager, HAST Co., Ltd. and President, HEMTCORE and 3D-bio Co., Ltd. Dr. Abe is a Fellow of IEEE. He received the Paper Award of the Laser Society of Japan in 1980, and the International Prize of SIOA in Italy in 1987. He is a board of the Japan Society of Applied Physics.



Hiroyuki Nagasawa received the B.E. M.E., and Ph.D. degrees Engineering from Tokai University, Japan in 1985, 1987, and 1997, respectively. After receiving Master degree, he worked at Toshiba Corporation as a semiconductor process engineer. From 1989, he was involved in development of x-ray lithography technologies in HOYA Corporation, and mainly concerned with thin-film formation of 3C-SiC. In 2002, he joined in HOYA Advanced Semiconductor Technologies (HAST) Co., Ltd.

as a chief-technology-officer (CTO), and is conducting developments of SiC material and devices.



Stefan Pothast received Dipl.Phys. degree from the University of Paderborn, Germany, in 2002. Currently he is performing his Ph.D. theses and works as Research Assistant at the University of Paderborn. His field of interest are molecular beam epitaxy of cubic group III nitrides and the development of cubic AlGaN/GaN high electron mobility transistors (HEMTs).



Jara Fernandez received her Master of Science degree from the University of Paderborn, Germany in 2005. Her field of interest is Schottky diodes on cubic group III-nitride semiconductors.



Jörg Schömann received Dipl. Phys. degree from the University of Paderborn, Germany, in 2002. Currently he is performing his Ph.D. theses and works as Research Assistant at the University of Paderborn. His field of interest are molecular beam epitaxy of cubic group III nitrides and the development of cubic AlGaN/GaN Quantum Well structures.



Donat Josef As received the Dipl.Ing. degree and the Dr. Techn. (Ph.D.) degree from the University of Linz, Austria, in 1982, and 1986, respectively. After a post-doc year at IBM research lab in Rüschlikon (Zürich, Swiss, 1987) he joined the Fraunhofer-Institute for Applied Solid-State Physics (IAF) in Freiburg, Germany, and the Heinrich-Hertz-Institute (HHI) in Berlin, Germany. In January 1995 he became Assistant Professor with the University of Paderborn, Germany. Since July 2001 he is Associated Professor at the Department of Physics, University of Paderborn and heads a group "Optoelectronic semiconductors – group III-nitrides." Currently he works in the field of molecular beam epitaxy and the development of electronic and optoelectronic devices of cubic group III-nitrides.



Klaus Lischka received the Dr. Phil. degree from the University of Vienna, 1973. From 1973 till 1994 he joined the Institute of Solid State Physics at University of Linz, Austria and headed a research institute for optoelectronics since 1989. Dr. Lischka was visiting Professor at the polish Academy of Sciences, at Philips netlab in Eindhoven and at Philips Analytical in Almelo/Netherland and received the AVL-LIST award 1991. Since 1994 he is full Professor at the Department of Physics, University of Paderborn and head of the group "Physics and Technology of Optoelectronic Semiconductors."